FZE-149
Dated 14 March 196

(1)

GDFW/D

401 237

MEASURED BARRIER INTERFERENCE ON MONOPULSE ANTENNA

(5) 351 860

GENERAL DYNAMICS | FORT WORTH

$2.60

(11) FZE-149
(9) 14 March 1963

(6) MEASURED BARRIER INTERFERENCE ON MONOPULSE ANTENNA

(7) NA

(8)
Prepared by: J. W. Landers

Approved by: Wm L Evans
W. L. Evans

Checked by: D. G. Harman
D. G. Harman

Checked by: L. H. Kidd
L. H. Kidd

(10) 25p. incl. illus. tables.

(12) NA

(13) NA

(14) Uncl

(15) NA

apc

TABLE OF CONTENTS

ABSTRACT

A Ku-band vertical monopulse antenna was tested for pattern distortion effects of a partial barrier within the antenna field. Barrier sizes were roughly equivalent to that of the reflector on the antenna. Primary effects noted were loss of gain in the sum pattern output and an angular shift in the central minimum of the difference pattern. Effects were limited to a relatively small region, and maximum pattern distortion occurred when the barrier was 3 to 4 degrees off the antenna boresight.

LIST OF FIGURES AND TABLES

Figures

Tables

INTRODUCTION

The objective of this study was the determination of the effect of a partial barrier within the field of a Ku-band vertical monopulse antenna. The physical barrier was a hemisphere made from an RF-absorbent material and was equivalent in size to the parabolic reflector of the test antenna. Specifically, hemispheres of 6, 8, and 10-inch diameter were used as barriers for an 8-inch diameter reflector. The spherical surface of the barrier faced the antenna.

The test antenna consisted of a dual Cutler feed arrangement, directed into an 8-inch diameter parabolic reflector, with the two feed outputs connected to the in-phase arms of a hybrid tee. The sum and difference outputs of the hybrid were detected and recorded as the antenna was rotated through a uniform field in the elevation plane.

Antenna radiation patterns were recorded, both with and without the barrier in place, for both sum and difference outputs. From these patterns, the effects of the barrier were determined for various barrier positions with respect to normal antenna boresight alignment. Significant effects were noted on sum pattern gain and difference pattern minimum level and angular position. These variations are tabulated and graphed in the form of contours as a function of the angular relationship between antenna boresight and the barrier. The actual radiation patterns are reproduced in drawings numbered GDA 105, 106, 107, 108, 109, 110 and 111.

TEST SETUP AND METHOD

A diagram of the antenna and barrier mounting on the antenna range model support is shown in Figure 1. The antenna was mounted on an auxiliary rotating pedestal, which, in turn, was attached to the normal azimuth table of the model support. The antenna was rotated 90 degrees from its normal mounting position to allow elevation plane patterns to be recorded with the model support rotating in the azimuth plane. The use of the auxiliary pedestal allowed the relative position of the barrier to be changed in elevation with respect to the normal antenna boresight. Azimuth position of the barrier was changed by sliding the dowel support rod of the barrier to a new position. Separation of the barrier from the front surface of the antenna reflector was effected as shown in Table 1.

Table 1 SEPARATION DISTANCES

Barrier Diameter (Inches)	Separation (Inches)
6	97
8	95
10	91

Barrier displacement angles are defined in Figure 2 with respect to antenna boresight, and Figure 3 is a block diagram of the antenna range pattern recording facilities.

The model support was moved out 30 feet from the transmitter antenna so that the barrier and the test antenna were in the far field. Reference patterns were recorded for both sum and difference outputs by rotating the barrier off 30 degrees from the

Note: The Azimuth Table, Auxiliary Pedestal and 2x4 Extension were covered with AN-73 "Eccosorb" to minimize reflections.

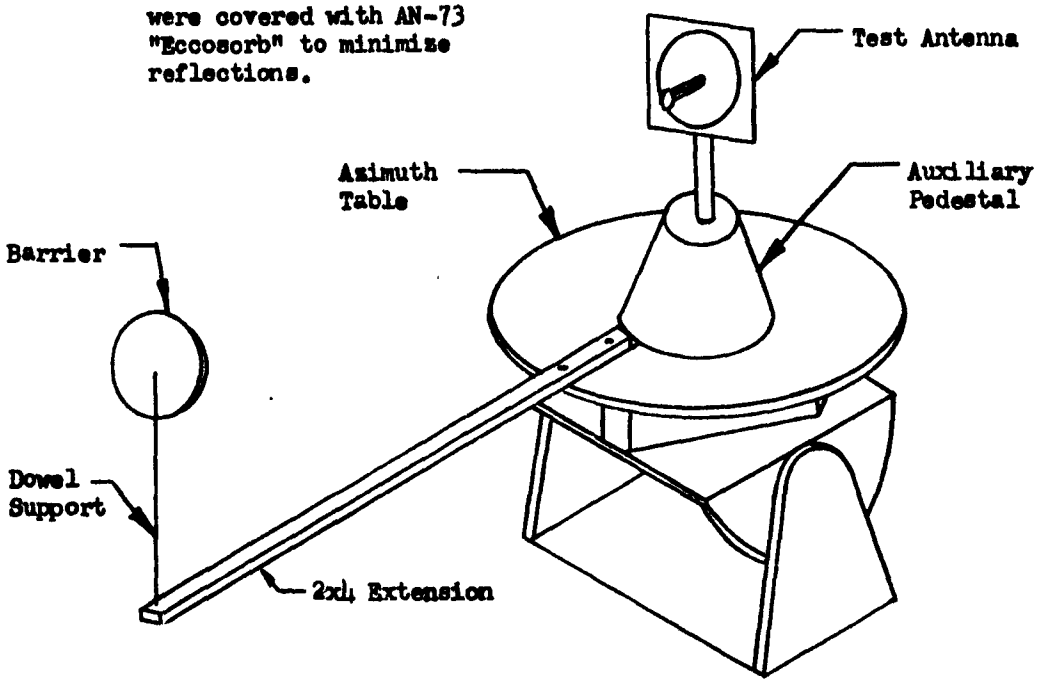

Fig. 1 ANTENNA AND BARRIER MOUNTING

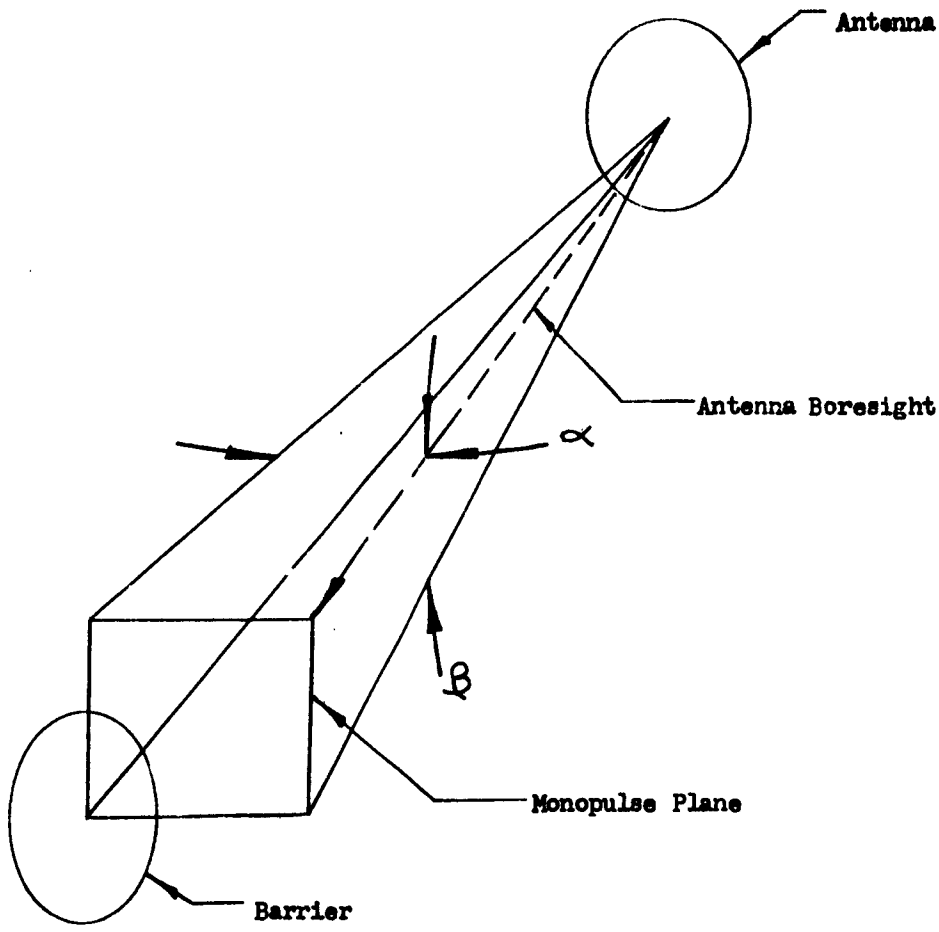

Fig. 2 BARRIER DISPLACEMENT DEFINITIONS

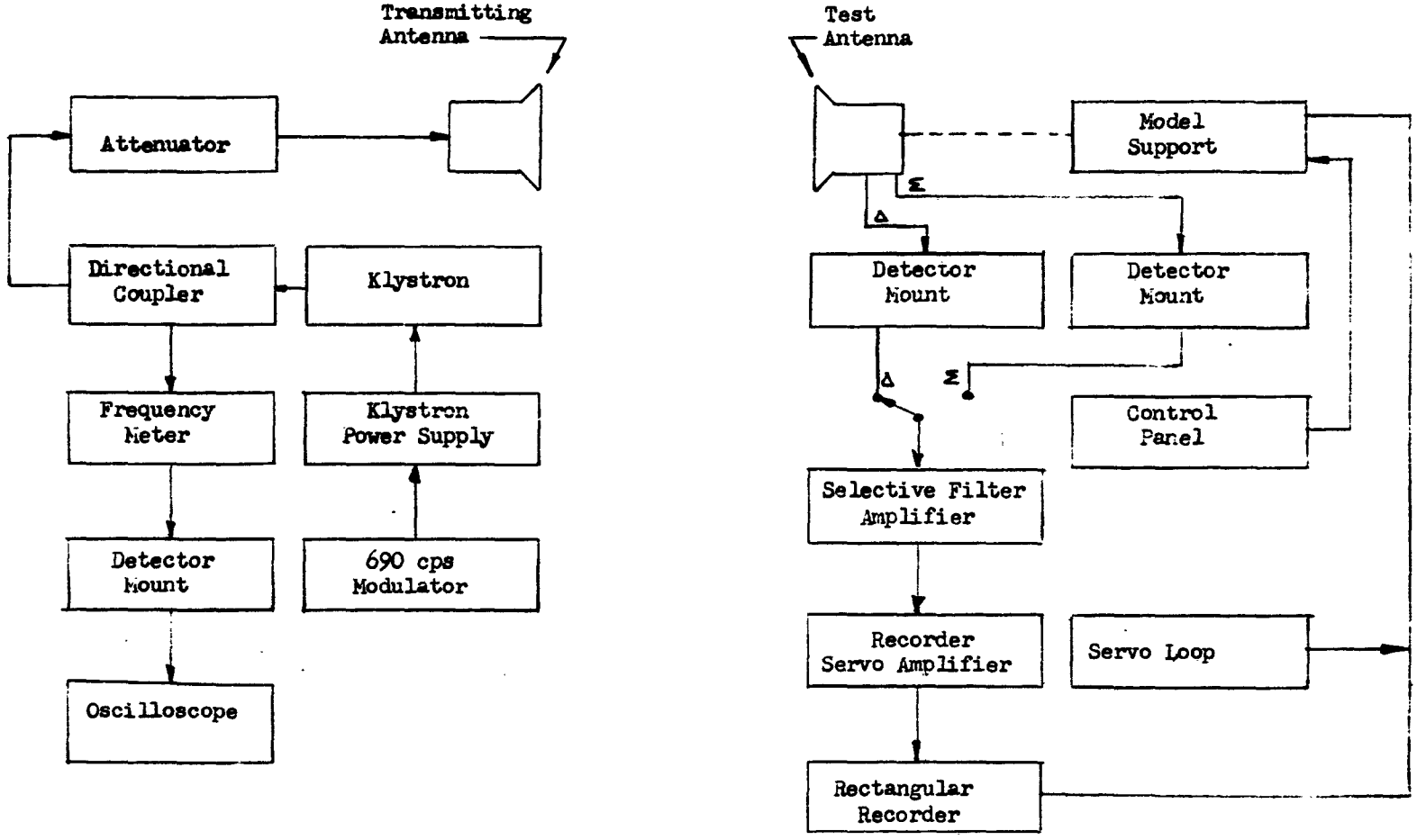

Fig. 3 BLOCK DIAGRAM OF ANTENNA PATTERN RANGE

boresight direction and rotating the antenna by use of the auxiliary pedestal. Interference patterns were then recorded by positioning the barrier in the desired location, rotating the azimuth table, and maintaining the desired relative location of the barrier. For data purposes, antenna boresight direction was defined as the position of the central minimum, commonly called the null, in the reference difference pattern. All angular displacements of the barrier were measured with respect to the boresight direction.

The detector mounts used on the test antenna outputs were identical types, but they were not balanced in terms of sensitivity. Therefore, no direct amplitude comparison can be made between sum and difference patterns. The only parameter affected by this lack of balance is the tabulation of the sum-to-difference amplitude ratio at the null.

Supplemental data were taken by maintaining a fixed position of antenna feed and barrier location and displacing the antenna beam by offsetting the dish reflector. In this case, the barrier position and method of beam displacement represented one proposed installation configuration. For comparison purposes, the 8-inch diameter hemisphere was covered with aluminum foil, and radiation patterns were recorded for $\alpha = 0$ degree and β variable between 0 and 10 degrees.

All data presented in this report were run at a frequency of 16.85 kilomegacycles. Checks were made at frequencies of 16.6 and 17.1 kilomegacycles with no change in results.

TEST RESULTS AND DISCUSSION

Elevation plane radiation patterns were recorded for barrier elevation angles β of 0, 1, 2, 3, 4, 5, 6, 8, and 10 degrees, and at barrier azimuth angles α of 0, 1, 2, 3, and 4 degrees. The patterns were recorded on an expanded elevation angle scale to facilitate interpretation, with the vertical scale directly in decibels. Patterns for the 6-inch hemisphere are shown in Drawing GDA-105, for the 8-inch hemisphere in Drawing GDA-106, and for the 10-inch hemisphere in Drawing GDA-107. Tables of Sum Pattern Gain Change, Difference Pattern Null Depth Change, Difference Pattern Null Shift, and Sum/Difference Ratio, as determined from the above patterns, are shown in Tables 1 through 3 for the three barriers. Contours of equal null shift for the three barriers are shown in Figures 4 through 6. Sum pattern gain change contours are shown in Figures 7 through 9. A positive null shift indicates that the actual direction of the beam occurs at a smaller elevation angle by the amount of the null shift indicated. Therefore, any position on the contour graphs which corresponds to a particular antenna boresight direction will have a beam direction whose elevation angle is less than the boresight elevation angle by the positive null shift angle.

A negative Null Depth Change indicates a null whose minimum is greater than the corresponding reference minimum. A negative Sum Gain Change indicates that the amplitude of the sum pattern is less than that of the corresponding reference pattern.

As previously mentioned, the detectors used for the sum and difference outputs were not balanced. The Sum/Difference Ratios tabulated in Tables 2, 3, and 4 were obtained by application of the corrections for Sum Gain Change and Null Depth Change to the 25 db nominal Sum/Difference Ratio applicable to this antenna as specified by the manufacturer.

Interference from the barrier is restricted to a relatively narrow region. The major contribution to pattern distortion, particularly in the region of the difference pattern null, appears to be the result of reflected energy from the barrier as it approaches the main beam of the antenna. This energy adds to and subtracts from the direct energy reaching the antenna and creates a periodic interference pattern.

The interference is most pronounced in the difference pattern in the region of the null. At this point, without any interfering object in place, the two feed outputs of the antenna are approaching equal amplitude and phase; when these outputs are combined in the hybrid tee, they produce a net output which approaches zero. The presence of an interfering object causes reflected energy of a rapidly changing phase to impinge on the feed and produces a net change in the output of the hybrid tee which causes the position of the null to change. In some cases, two distinct nulls are formed, and in others a general "filling" of the null occurs so that a relatively broad null region is produced. In addition to the more dramatic changes noted here, in many instances the smaller null shifts (0.1 to 0.3 degree) are accompanied by rather drastic positive and negative changes in the null depth. Null depth changes of 6 to 8 db are not uncommon. The effects of the

barrier on the sum pattern are somewhat less pronounced, but they are readily apparent in the patterns. Some loss in gain due to aperture blocking is inevitable.

The primary source of error in a monopulse radar system caused by a barrier, such as the one simulated for these tests, would be the angular shift in null position. Some performance degradation would be caused by loss in antenna gain, and loss in null depth is significant, but only if the differential in sum pattern output and null depth required for proper system operation is not maintained. In the tables and contour plots, the data on null shift is presented in terms of an amplitude position shift only, without regard to the relative phases of the sum and difference outputs. The use of phase comparison techniques was attempted for this test, but the results were not conclusive and are not included. Some difference in results might be expected if a phase comparison were made, but it is felt that the difference would be slight and that the same character of null shift would result.

For comparison purposes, the 8-inch diameter hemisphere was covered with aluminum foil and the condition $\alpha = 0$ degrees and variable between 0 and 10 degrees was rerun. Reflections from the foil surface are larger, and the effects on the patterns are more pronounced. These patterns, shown in Drawing GDA-108, may be directly compared with those in GDA-106 for the uncovered barrier. This comparison indicates that the foil contributes to a larger null shift but that the trend of the error remains the

same. It was not possible to apply a perfectly smooth covering of foil to the barrier, and the resultant wrinkling of the surface may have exaggerated the effect.

All data thus far presented was taken with the entire test antenna rotated on its mounting pedestal to provide a variable position of the barrier for ease of operation and, by using the antenna range remote servo system, to provide a reference position which could be easily maintained. However, this particular antenna was designed to provide elevation beam displacement by maintaining the feed assembly at boresight and deflecting the beam by gimbaling the dish reflector. To assure that the patterns presented were valid, data were taken to provide a comparison of the two methods of beam deflection. Patterns for the 8-inch diameter hemisphere were recorded for $\beta = 2$, 3, and 4 degrees and $\alpha = 0$ degrees. These patterns were repeated by resetting the antenna assembly to boresight and deflecting the beam by an equivalent amount ($\gamma = 2$, 3, and 4 degrees, with $\alpha = 0$ degrees). Comparison of these two sets of patterns indicates good correlation and validates the method used for the patterns presented. Both sets of patterns are shown on Drawing GDA-109.

It was desired to obtain some specific data on one possible installation configuration for antenna barrier position. Two barrier positions were chosen; they were defined by angular displacements of $\beta = 6.6$ degrees, $\alpha = 0$ degrees and $\beta = 6.6$ degrees and $\alpha = 3$ degrees, and the antenna-to-barrier separation of each was 95 inches. For these conditions, beam displacement in the elevation plane was obtained by dish displacement. Beam deflection

angles δ of 0 to 18 degrees were run for the first condition; the patterns are shown on Drawing GDA-110. Patterns for the second configuration, with δ variable from 0 to 12 degrees, are shown in Drawing GDA-111. Direct comparison of these patterns with specific patterns previously presented cannot be made, but their characteristics can be located on the contour graphs to prove that the two methods of deflecting the beam yield similar results.

CONCLUSIONS

Some undesirable effects are noted in the radiation patterns of a vertical monopulse antenna when a partial barrier is within the field of the antenna. The region of influence is relatively small. The primary effects are loss of gain in the sum output, caused partly by aperture blocking, and an angular shift of the difference output null because energy reflected by the barrier unbalances the inputs to the hybrid tee. Application of this data to a particular system or installation must be made with regard to the intended function of the system and its accuracy and safety limitations, and some consideration must be given to other potential sources of error or degradation.

Table 2 TABULATED DATA FOR 6-INCH DIAMETER BARRIER

NULL SHIFT (DEGREES)

	0	1	2	3	4	6
0	+ .1	0	+ .1	+ .2	0	+ .2
1	+ .1	+ .6	+ .5	+ .3	+ .1	+ .2
2	+ .9	+1.0	+ .6	+ .5	+ .2	+ .1
3	+ .8	+1.3	+1.1	+ .3	+ .2	
4	+1.5	- .4	- .5	- .2	+ .1	
5	- .4	- .3	- .3	0	+ .2	
6	0	- .1	- .2	+ .2	0	
8	+ .3	+ .4	+ .3	+ .3	0	
10	0	+ .3	+ .2	+ .1		

NULL DEPTH CHANGE (db) N

	0	1	2	3	4
	+ 4.6	- .5	- 1.5	- 1.7	- 2.0
	- 5.8	- 8.7	- 6.0	+ .1	+ 4.8
	- 8.2	- 9.5	- 3.9	+ 6.3	+ 1.5
	- 4.4	- 3.5	+ 8.4	- 8.6	+ .3
	+ .2	+ 3.7	+ 9.4	+ 1.8	+ 3.0
	- .1	+ .3	+ .1	+ 1.4	- 4.5
	- 4.1	- 4.8	- 5.5	- 4.2	- 7.8
	+ 5.6	+ .5	+ 5.6	+ 5.3	+ 4.0
	- .4	- 2.9	- .6	+ .8	+ .6

SUM GAIN CHANGE (db) G

0	-2.6	-2.5	-3.4	-3.7	-2.8	0
1	-3.0	-2.9	-3.8	-3.8	-2.5	0
2	-3.7	-3.9	-4.2	-2.9	-1.7	0
3	-4.7	-4.3	-3.4	-2.0	- .3	
4	-3.7	- .6	- .6	- .3	+ .4	
5	- .9	- .2	0	+ .5	+ .4	
6	- .6	+ .1	- .3	+ .2	- .2	
8	- .9	- .3	- .3	- .1	- .2	
10	- .1	- .4	- .3	- .3		

SUM/DIFFERENCE RATIO (db) S/D

27.0	22.1	20.1	19.6	20.2
16.2	14.4	15.2	21.3	27.3
13.1	11.6	16.9	28.4	24.8
15.9	17.2	30.0	14.4	25.0
21.5	21.9	33.8	26.5	28.4
24.0	25.1	25.1	26.9	20.9
20.3	20.3	19.2	21.0	17.0
29.7	25.2	30.3	30.2	28.8
24.5	21.7	24.1	25.5	

$S/D = 25\ db + G + N$

Table 3 TABULATED DATA FOR 8-INCH DIAMETER BARRIER

NULL SHIFT (DEGREES)

	0	1	2	3	4	6
0	+ .1	+ .2	- .1	+ .1	0	- .1
1	+ .5	+ .8	+ .6	+ .8	+ .5	0
2	+1.0	+1.1	+1.1	+1.2	+ .9	+ .1
3	+1.2	+1.6	+1.5	+1.1	+ .7	- .2
4	+2.1	+2.1	+1.9	+1.3	+ .2	0
5	+ .2	+ .1	+ .3	- .1	- .1	- .1
6	- .3	- .3	- .1	- .2	- .3	+ .1
8	+ .2	+ .3	+ .2	0	+ .1	- .1
10	+ .1	+ .1	+ .1	+ .1	- .1	+ .1

NULL DEPTH CHANGE (db) N

	0	1	2	3	4	6
0	+ 3.3	+ .1	+ .3	+ 3.5	- .1	- .8
1	- 7.7	- 8.3	- 8.8	- 4.9	+ .2	+ 1.2
2	-12.4	-11.2	-13.6	- 6.3	+ 4.4	+ .9
3	-10.4	- 8.3	-11.6	- 2.0	+ 2.3	+ 2.9
4	+ 5.9	+ 4.2	+ 4.5	- 5.0	- 1.0	- .7
5	- 2.9	- 2.0	- 4.1	- 2.1	+ .8	- 5.9
6	0	- 8.6	- .7	+ 2.6	- 3.1	- 7.3
8	- 7.3	- 6.8	- 7.9	- 7.1	- 4.7	+ 2.9
10	- 4.8	- 4.4	- 3.4	- 3.3	- 1.8	- 4.1

GAIN CHANGE (db) G

	0	1	2	3	4	6
0	-4.5	-4.3	-3.4	-3.9	-4.7	-1.2
1	-4.3	-3.7	-3.3	-3.6	-4.0	-1.2
2	-5.1	-4.8	-3.6	-3.8	-4.4	- .8
3	-5.8	-5.0	-4.4	-4.1	-3.7	+ .1
4	-4.8	-3.9	-3.6	-1.6	-1.2	+ .2
5	+ .2	+ .2	0	+ .3	+ .1	+ .4
6	+ .8	+ .3	+ .9	+ .9	0	- .2
8	- .2	- .2	0	+ .4	- .3	- .3
10	0	- .5	0	+ .4	- .5	- .2

SUM/DIFFERENCE RATIO (db) S/D

	0	1	2	3	4	6
0	24.2	20.8	21.9	24.6	20.2	23.0
1	13.0	13.0	12.9	16.5	21.2	25.0
2	7.5	9.0	8.1	14.9	25.0	25.1
3	13.8	11.7	9.0	18.9	23.6	28.0
4	26.1	24.2	25.9	18.4	22.8	24.5
5	22.3	23.2	20.9	23.2	25.9	19.5
6	25.8	16.7	25.2	28.5	21.9	17.5
8	17.5	18.0	17.1	18.3	20.0	27.6
10	20.2	20.1	21.6	22.1	22.7	20.7

$S/D = 25 \text{ db} + G + N$

Table 4 TABULATED DATA FOR 10-INCH DIAMETER BARRIER

NULL SHIFT (DEGREES)

	0	1	2	3	4	6
0	+ .1	+ .1	- .1	- .1	+ .2	+ .1
1	+ .9	+ .7	+ .4	+ .7	+ .2	+ .2
2	+1.6	+1.5	+ .7	+ .8	+ .3	+ .1
3	+1.9	+1.8	+ .7	+ .9	+ .3	+ .1
4	+2.5	+ .8	+ .8	+1.1	- .2	+ .1
5	+1.1	+ .3	0	+ .4	0	
6	- .1	- .1	- .3	- .2	+ .2	
8	+ .3	- .1	- .1	+ .4	+ .5	
10	+ .2	+ .2	0	+ .3	+ .3	

NULL DEPTH CHANGE (db) N

	0	1	2	3	4
0	+ 6.1	+ 4.3	+ .1	- 7.0	- 1.9
1	- 2.6	+ 2.5	+ 5.2	- 1.5	+ 4.7
2	-10.6	+ 1.3	- .6	+ 4.2	+ 2.1
3	- 9.8	+ 1.9	- 2.2	+ 2.7	- .1
4	+ 4.1	+ .2	- 4.3	- 3.3	+ 3.6
5	- 4.6	- 7.7	- 8.2	- 6.9	+ 3.3
6	- .5	- .9	+ 4.5	+ .1	- 8.3
8	-10.5	- 7.9	- 9.4	-11.9	- 6.2
10	+ 5.7	+ 1.6	+ 4.8	+ 1.0	- 4.3

CAIN CHANGE (db) G

	0	1	2	3	4	6
0	-6.9	-9.4	-7.5	-4.1	-3.1	+ .2
1	-6.8	-8.8	-6.8	-4.7	-2.8	+ .5
2	-6.9	-8.3	-6.1	-4.3	-2.2	+ .6
3	-6.5	-6.5	-4.5	-3.4	-1.1	+1.2
4	-6.1	-3.1	-2.8	-1.7	+ .7	+1.2
5	-2.8	+ .3	+ .1	-1.0	+1.9	
6	+ .2	+ .9	+1.1	+ .6	+1.8	
8	- .3	+ .3	+ .2	+ .6	+ .9	
10	- .3	+ .8	+ .2	+ .2	+1.2	

SUM/DIFFERENCE RATIO (db) S/D

	0	1	2	3	4
0	24.2	19.9	17.6	13.9	20.0
1	15.6	18.5	23.4	17.8	26.9
2	7.5	18.0	18.3	24.9	24.9
3	8.7	20.4	18.3	24.3	23.8
4	23.0	22.1	17.9	20.0	29.4
5	17.6	17.6	16.9	17.1	30.2
6	24.7	25.0	30.6	25.7	18.5
8	14.2	17.4	15.8	13.7	19.7
10	30.4	27.4	30.0	26.2	21.9

$S/D = 25\ db + G + N$

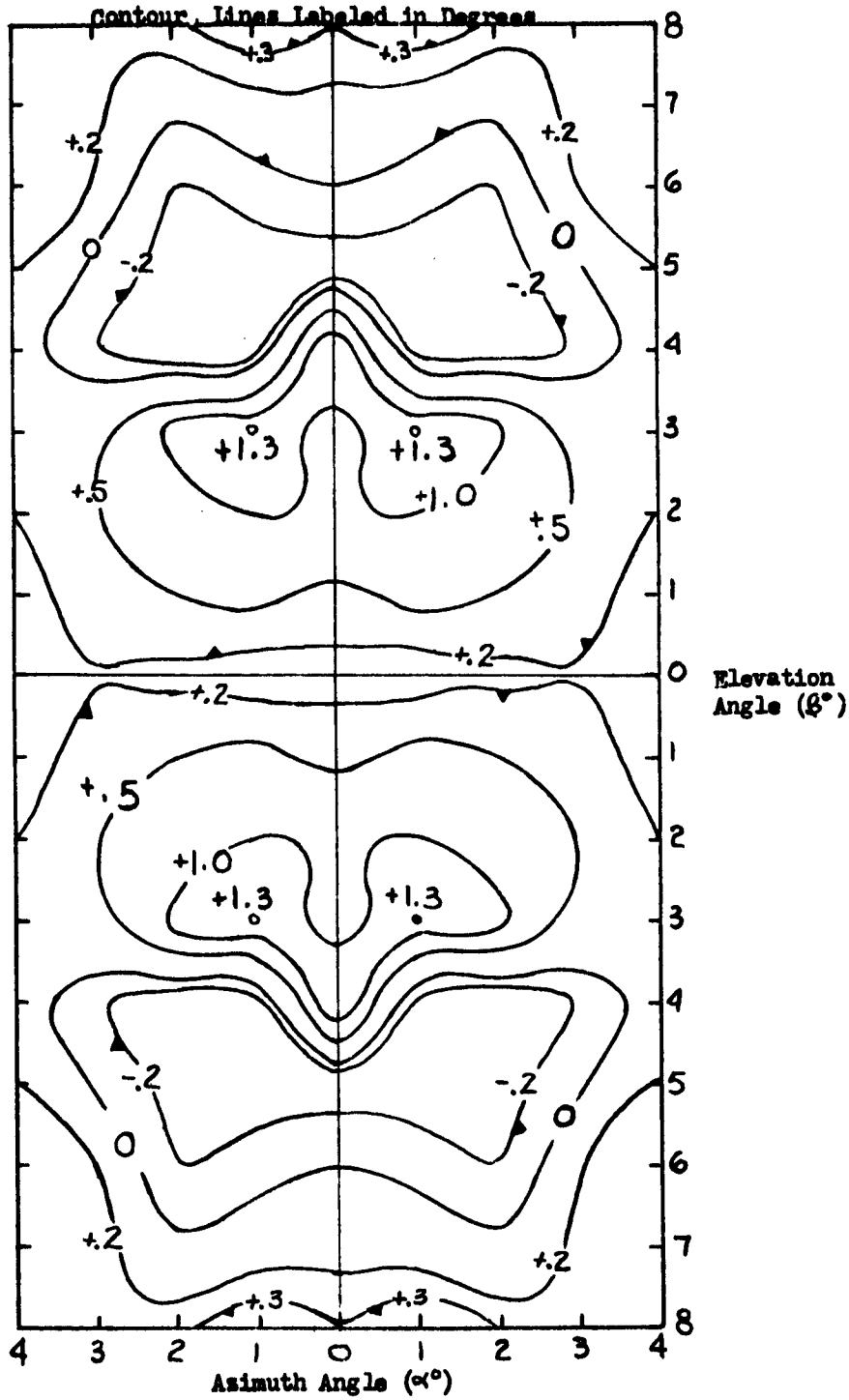

Fig. 4 NULL SHIFT CONTOURS, 6-INCH DIAMETER BARRIER

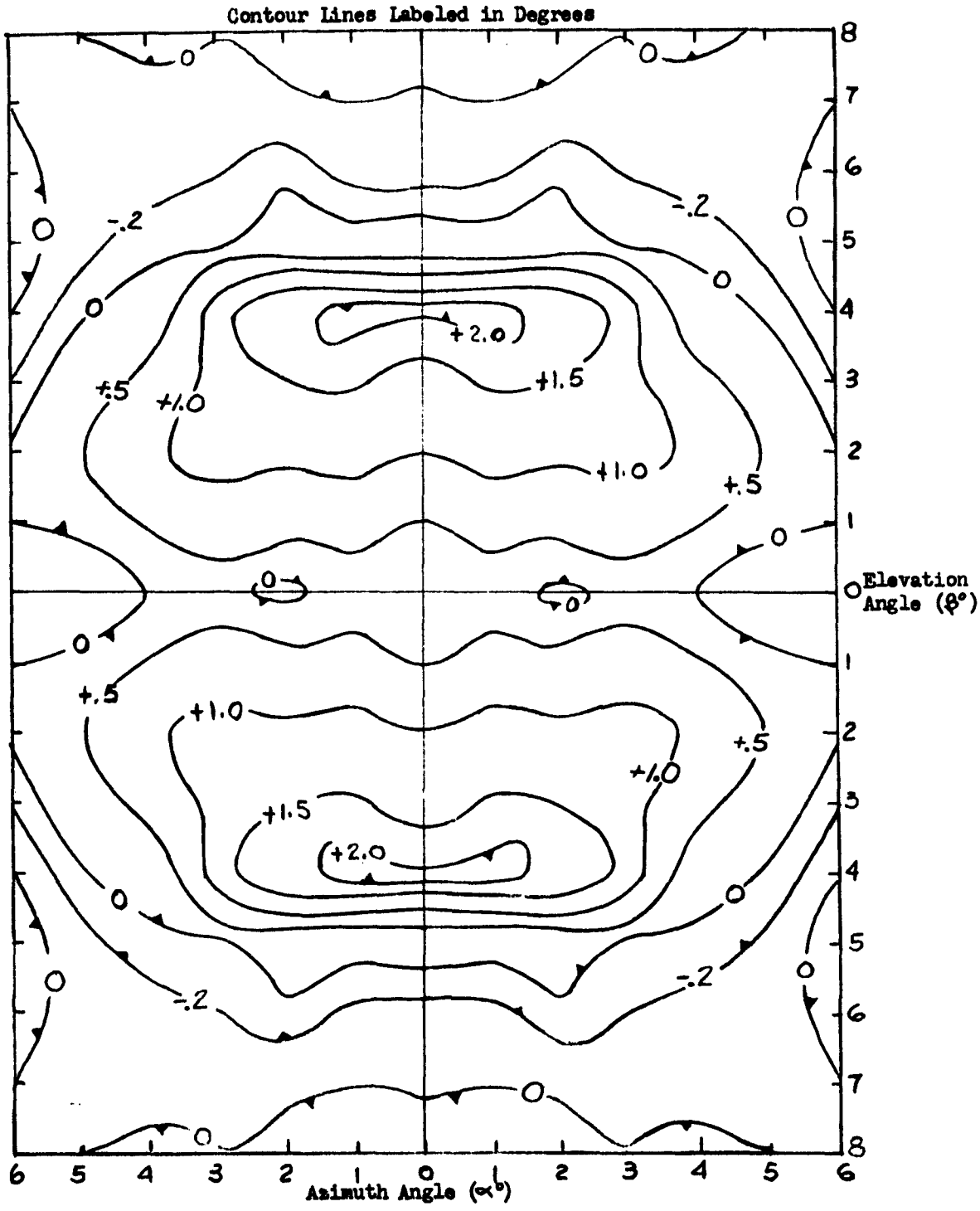

Fig. 5 NULL SHIFT CONTOURS, 8-INCH DIAMETER BARRIER

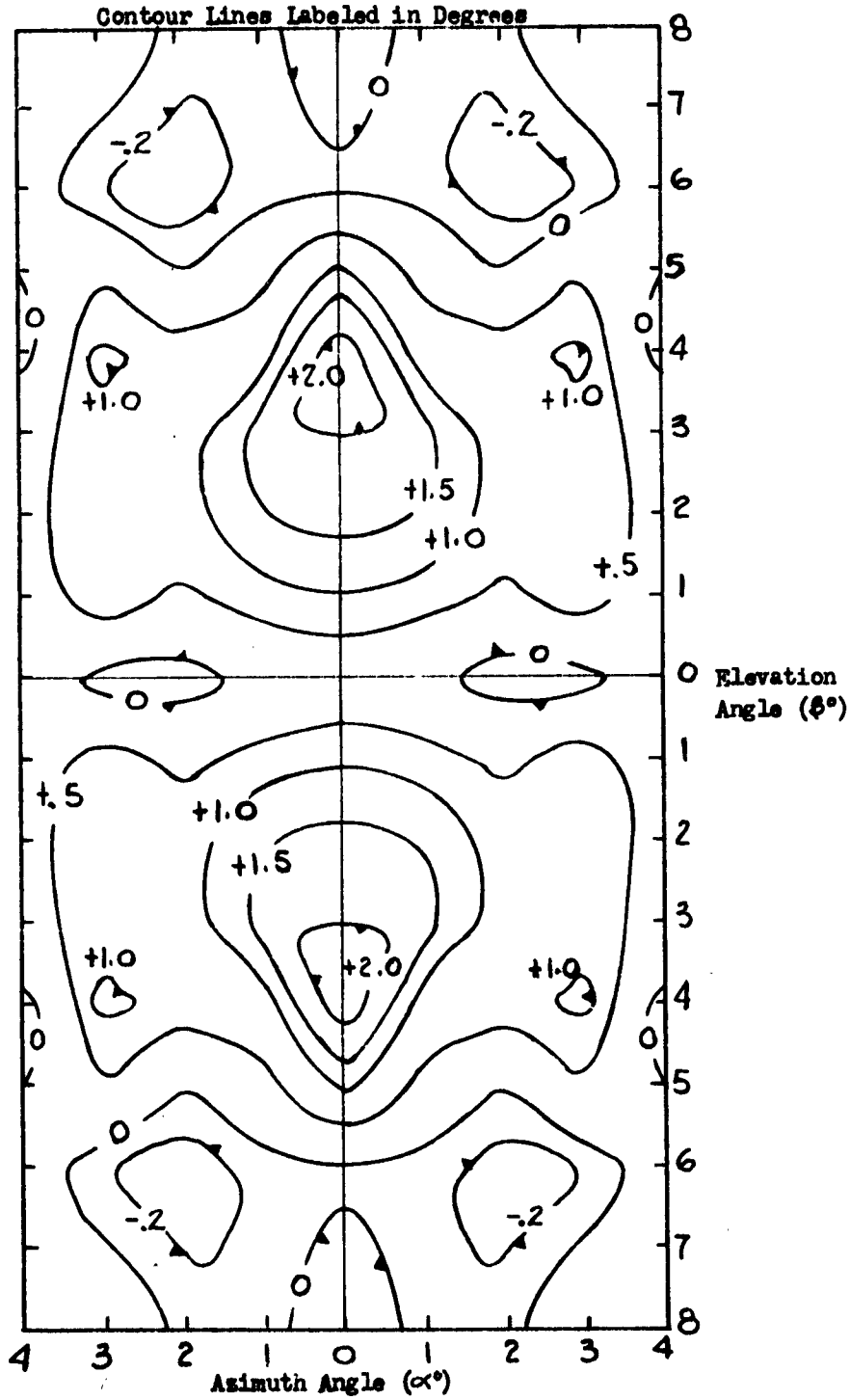

Fig. 6 NULL SHIFT CONTOURS, 10-INCH DIAMETER BARRIER

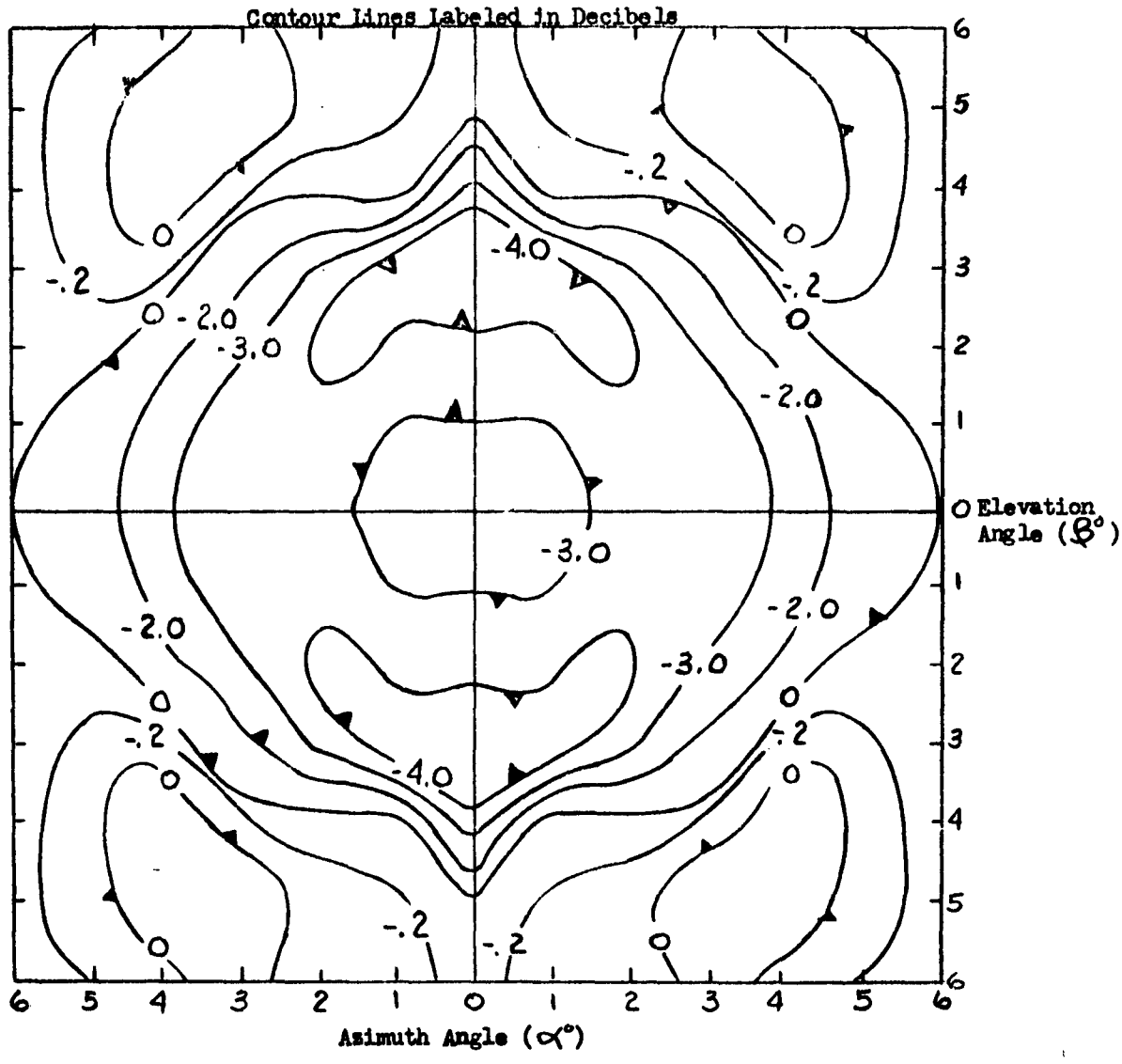

Fig. 7 GAIN LOSS CONTOURS, 6-INCH DIAMETER BARRIER

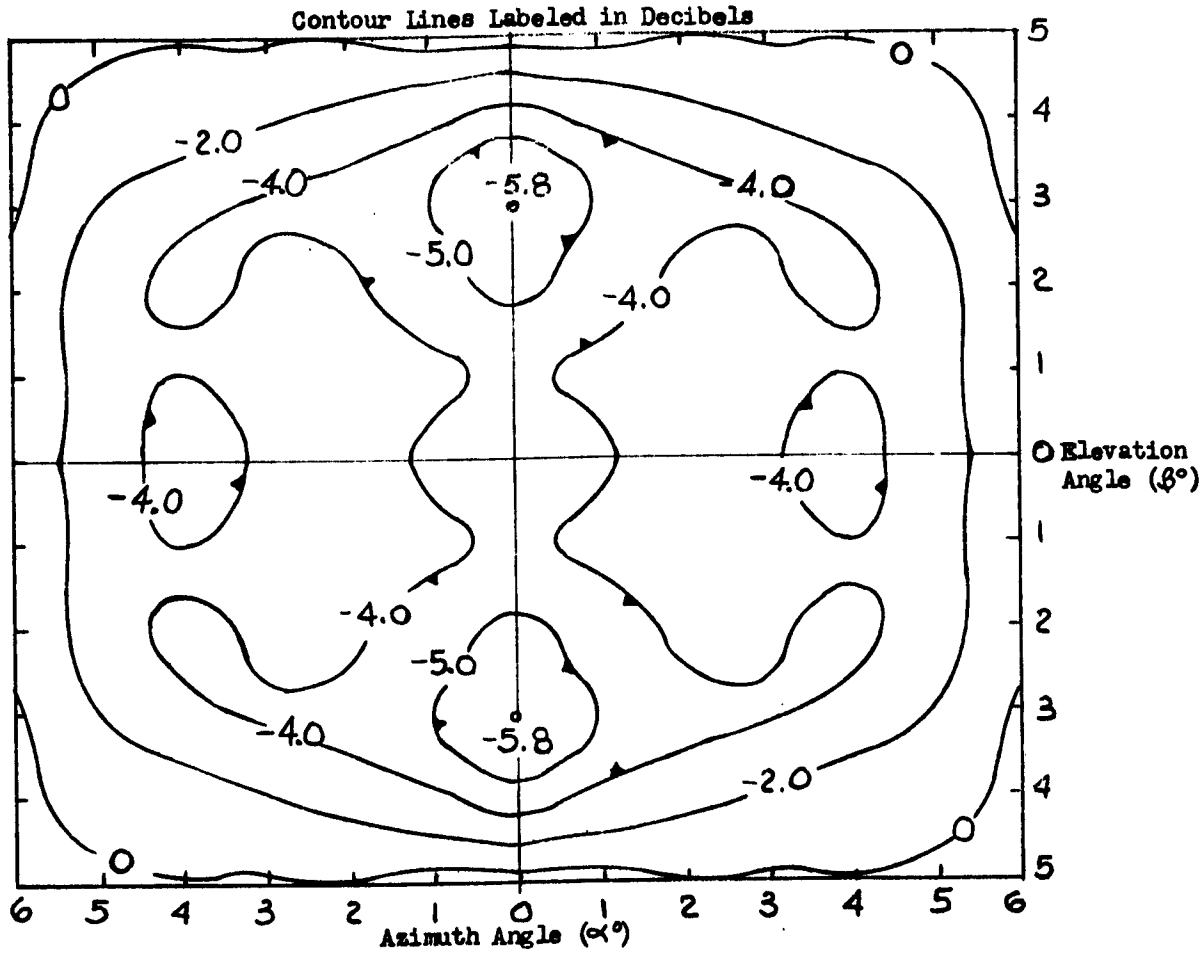

Fig. 8 GAIN LOSS CONTOURS, 8-INCH DIAMETER BARRIER

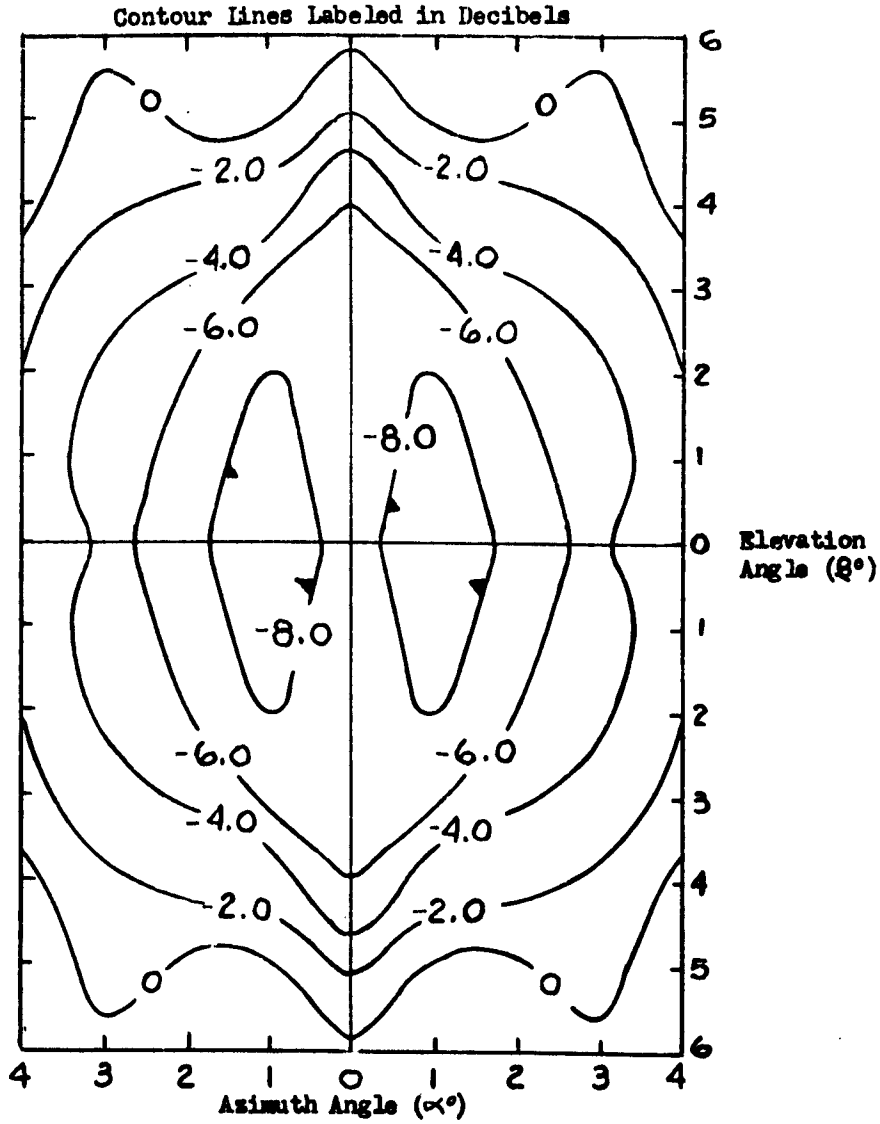

Fig. 9 GAIN LOSS CONTOURS, 10-INCH DIAMETER BARRIER